# INFLUENCE OF TURBULENCE MODELLING ON THE SIMULATION OF A PASSIVELY-CONTROLLED TRANSONIC CAVITY FLOW

**Ivan Mary**
ONERA, 29, avenue de la Division Leclerc 92322 Châtillon Cedex, France
Ivan.Mary@onera.fr
**Frédéric Daude**
ONERA, 29, avenue de la Division Leclerc 92322 Châtillon Cedex, France
Frederic.Daude@onera.fr
**Pierre Comte**
LEA, Laboratoire d'Etudes Aérodynamique
UMR6609 CNRS, Univ. Poitiers, ENSMA, France
pierre.comte@lea.univ-poitiers.fr

## ABSTRACT

Simulations of a high-subsonic open-cavity flow controlled by a spanwise rod are presented. The $30dB$ reduction of the peak pressure tone and the reduction by $6dB$ of the background pressure found in comparable experiments performed at ONERA are retrieved. The injection of deterministic upstream fluctuations in the LES domain is found to be of crucial importance, in contrast with the baseflow case. Reduction of the vortex impingement onto the aft edge of the cavity is confirmed, together with reduction of mass flow rate breathing through the grazing plane. Visual evidence of merging between the Kelvin-Helmholtz-type vortices shed downstream of the fore edge of the cavity and the von Kármán vortices shed behind the cylinder is provided. Shocklets downstream of the cylinder are also observed.

## INTRODUCTION

The high levels of pressure tones caused by compressible flows over open cavities have motivated considerable efforts, in order to understand the underlying physical mechanisms and develop control strategies which are effective not only for a specific design point, but also for a sufficiently wide range of parameters around it to be of practical interest.

It is well established that grazing flows over open cavities, namely, cavities too short for the recirculation zone past the upstream edge to close, develop unsteadiness due to some coupling between the reattachement region near the aft edge and the region where the incoming boundary layer detaches, past the upstream edge. Conceptual models developing self-sustained oscillations exist in the incompressible limit (Howe 1997), featuring Biot-Savart-type instantaneous interaction. Pressure tones are found, the frequencies of which scale on the inverse of the cavity length $L$, and which are enharmonic up to an end correction $\gamma$ as customary in impinging flows (Powell 1961),(Rockwell and Naudascher 1978). These models can be extendend to weakly compressible flows, as in (Chatellier et al. 2004). At higher Mach number, the propagative nature of the coupling has to be taken into account. The interaction is referred to as "fluid-acoustic mode" in (Rockwell and Naudascher 1978), in contrast with the "fluid-fluid mode" that prevails at vanishing Mach number. Assuming that the frequency of shedding of the Kelvin-Helmholz vortices matches that of acoustic waves propagating upstream within the cavity yields the Rossiter model $f_n = \frac{U_\infty}{L}\frac{n-\gamma}{M+\frac{1}{\kappa}}$, in which $M = U_\infty/a$ denotes the external Mach number and $\kappa = U_c/U_\infty$ involves an average convection speed of the Kelvin-Helmholtz vortices (Rossiter 1964). A broad set of experimental configurations provided values for both constants $\kappa$ and $\gamma$ as a function of the length-to-depth aspect ratio $L/D$ of the cavity, and the model has proved to match quite well frequencies of the pressure tones, up to some ad-hoc tuning of both parameters. However, attempts to educe a universal behaviour of cavity flows have not been successful, because of the observed influence of the following parameters on the receptivity of the detached mixing layer: $L/D$, but also $L/W$, $L/\theta$ and the flow parameters $Re_\theta$, $M_\infty$, the shape factor of the incoming boundary layer $H = \delta^*/\theta$ and the overall pressure level $p_{rms}/q_\infty$ within the cavity (Cattafesta et al. 2003). This sensitivity not only to the level of the tones but also to the broad-band noise makes the prediction and the optimization of control strategies particularly challenging (see (Cattafesta et al. 2003, Rowley and Williams 2006) for a review).

The motivation here is focussed on the assessment of the needs of numerical insight to reproduce quantitatively the unsteadiness reduction effects of a simple passive actuator, in the simplest possible high-subsonic cavity configuration: such a low aspect ratio as $L/D = 0.42$ is considered, as in (Forestier et al. 2003, Larchevêque et al. 2003) in order to minimize large-scale three-dimensional effects. The control device considered is a spanwise cylinder placed in the upstream boundary layer, as proposed in (McGrath and Shaw 1996). This was proved to reduce significantly both the tone and broadband pressure levels, provided the diameter $d$ and its height[1] $y$ are suitably chosen. One of the key enablers for this so-called High-Frequency Tone Generator is the Reynolds number independence of the cylinder's wake Strouhal number $St = fd/U_\infty \sim 0.2$. A detailed experimental investigation (Illy 2005, Illy et al. 2004) performed at ONERA for different $L/D$, boundary layer thicknesses, and Mach numbers ranging from 0.6 to 0.78, concluded that the main parameter is the ratio $y/d$, with an optimum at $y/d = 1.2$ yielding a reduction by 30dB and 6dB of the peak tone and the overall pressure *rms*, respectively, and this despite the added noise of the cylinder. In contrast with the baseline case, it was found that $p_{rms}$ did not increase with $M$, hence a highest efficiency found at the highest $M$ possible with the experimental facility before the onset of sonic choking effects, *viz.*, $M = .78$.

---

[1] here defined as in (Forestier et al. 2003, Larchevêque et al. 2003), as the clearance between the bottom of the cylinder and the wall

Here, two calculations will be compared, differing essentially in the treatment of the incoming boundary layer. The numerical details are given in the next section. The results of both calculations are compared in section , in which pressure and velocity statistics are presented together with visualisations. The contribution of this investigation to the current understanding of this intriguing feedback loop will eventually be summarized.

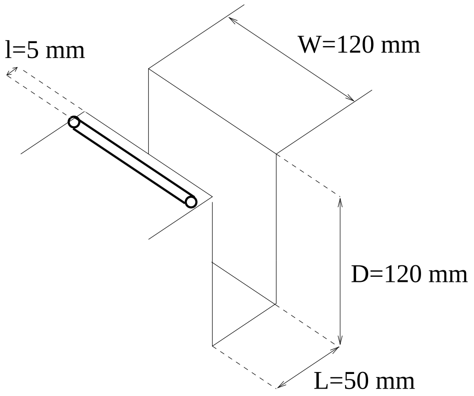

Figure 1: Sketch of the cavity and the cylinder

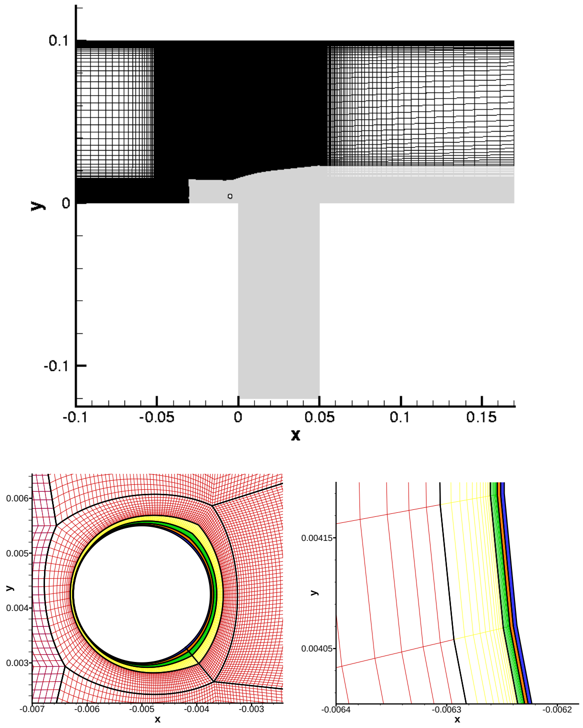

Figure 2: Section $(x, y)$ of the grid: general view, for the LES (top). Zoom near the cylinder (bottom, left and right, resp., same for both calculations)

## COMPUTATIONAL SETUP

The numerical methodology employed here has been adapted from (Larchevêque et al. 2003) (see also (Larchevêque et al. 2004, Larchevêque 2003) for other aspect ratios), for which very good agreement with the experimental counterparts was found, in particular regarding the pressure levels and the dynamics of the phase-averaged coherent structures. In this $L/D = 0.42$ case, the overall large-scale two-dimensionality of the flow makes it possible to use 2D URANS in the portions of the flow where the boundary layer is attached, and devote most of the computing power to the matched Large-Eddy Simulation of a streamwise portion of the flow, in a 3D domain of span $W_{num} = L$ with periodic boundary conditions, whereas the span $W = D$ of the experimental test section is 2.4 times as large. The Reynolds number based on the length L of the cavity is $8.21 \times 10^5$, as in the experiment.

The major difficulty on the numerical side is to account for the cylinder, which is of diameter $d = 2.5$ mm, whereas the thickness of the incoming boundary layer is $\delta_{99\%} = \delta = 9.8$ mm. The thickness of the boundary layer cylinder is smaller than $0.1mm$. Turbulent boundary layers have to be gridded with a wall-normal resolution of about one wall unit. In fact, $y^+_{min} \sim 2$ proved to be sufficient, either in URANS or LES. The block-structured grid shown in Fig. 2 has about $\sim 20\ 10^6$ grid points, and meets the LES requirements $\Delta x^+ \sim 50$, $\Delta y^+ \sim 2$, $\Delta z^+ \sim 20$. The cavity length is discretized over about 200 meshes, and there are 256 points in the spanwise direction, with $W_{num} = 20\ d$, that is, 5 times as much as in the incompressible cylinder wake simulations (Kravchenko and Moin 2000). In the LES, the 3D zone is preceded by a box of width $W_{num}/5 = 4\ d$ replicated 5 times in the spanwise direction, and in which the incoming boundary layer and its fluctuations are generated by means of a recyling method inspired by (Lund et al. 1998) and adapted to compressible RANS-LES interfacing. We are aware that this spanwise replication, motivated by CPU time considerations, could be critized because it deprives the upstream forcing of spanwise scales significantly larger than the spanwise integral scale of the turbulence generated by a canonical wake in a turbulence-free environment. Nevertheless, $W_{num}/5 = 4\ d$ is large enough for the dominating instabilities of the wake to develop, as in (Kravchenko and Moin 2000).

The SubGrid-Scale model used in the LES portion (in pale in the left plot of Fig. 2) is the Selective Mixed-Scale model proposed in (Lenormand et al. 2000). The dark regions are treated in 2D URANS, with the Spalart-Allmaras model, as in (Larchevêque et al. 2003). In that paper, the injection of realistic upstream fluctuations was not found to be needed for recovery of correct results in the baseline configuration. A repetition of it with the cylinder has thus been undertaken, with the same grid as described above, except that the region upstream of the cylinder is treated in 2D URANS. Because it switches from URANS to LES, this calculation will be hearafter referred to as DES , although the switching is monitored by the multi-block decomposition and not by comparison between the mesh size and the local turbulence integral scale.

Implicit time integration is used, as in (Larchevêque et al. 2004), but with a block-local determination of the number of iterations of the Newton-type inner process designed in such a way that the balance of the convergence errors is ensured despite the high gradient of CFL number near the cylinder. Consistency with results obtained with time-explicit schemes has been assessed in the case of the linear advection of a 2D vortex and in the case of the low Mach number flow on an airfoil at moderate angle of attack, near the recirculation bubble on the leeside (Daude et al.).

Table 1 highlights the computational effort and the mesh size discrepancies. The CPU times mentioned correspond in each case to 50 periods of the fundamental Rossiter mode

|  | Number of cells ($\times 10^6$) |  |  | $\Delta t(\mu s)$ | CPU |
|---|---|---|---|---|---|
|  | $\sigma \leq 16$ | $\sigma \leq 700$ | total |  |  |
| Bsl. | 1.6 | / | 1.6 | 1.4 | 40 |
| LES | 20 | 0.5 | 20.5 | 0.25 | 2200 |
| DES | 17 | 0.5 | 17.5 | 0.25 | 1316 |

Table 1: Mesh and computational parameters for cavity simulations. Bsl refers to the baseline simulations of (Larchevêque et al. 2003)

(*i.e.* 0.025$s$), computed on a NEC SX6 with an average speed of 4 Gflops per processor.

## RESULTS ANALYSIS

Figure 3 shows the organized vortices educed by means of a positive Q surface. Both the DES and the LES develop Kelvin-Helmholtz and von-Kármán-type vortices in between which streamwise vortices are stretched. The LES shows a higher level of small-scale turbulence. The corresponding movies show less large-scale unsteadiness in LES than in DES , with low-frequency flapping of the mixing layer dramatically reduced with respect to the baseline configuration, without the cylinder, which is consistent with (Illy et al. 2004) and other experimental references. In particular, the impingement of spanwise-organized large scale vortices on the aft edge of the cavity and the trapping events are visibly inhibitted by the presence of the cylinder.

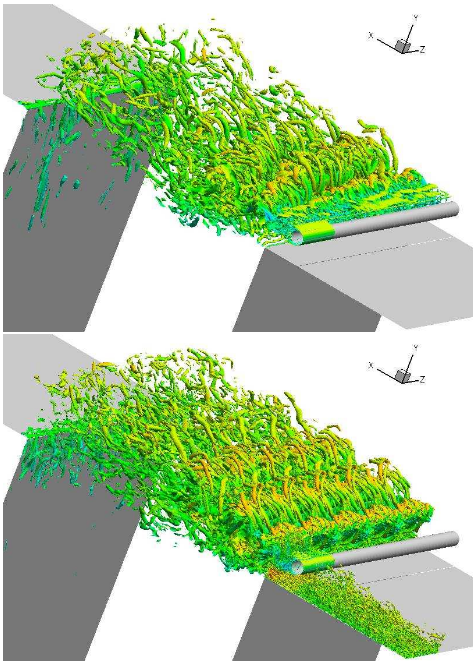

Figure 3: Isosurfaces of $Q = 2\ (U_\infty/d)^2$ coloured by the streamwise velocity. DES (top), LES (bottom).

The pressure spectra (Fig. 4) recorded on the rear wall of the cavity at $y/D = -0.08$ show more differences between the LES and the DES than the visualizations: the LES reproduces satisfactorily the reduction of the first Rossiter mode at 2$kHz$ and that of the next ones observed in (Illy et al. 2004). In contrast, the DES shows much less reduction of the tone levels, which shows the influence of the upstream boundary layer fluctuations. However, both calculations underestimate the peak at 20$kHz$ due to the wake of the cylinder, by almost 10$dB$. They also underpredict the width of this peak, which is significantly wider than that of the Rossiter tones, but one should keep in mind that the pressure signal is recorded 20 diameters downstream of the cylinder, which is quite demanding in terms of resolution and numerical dissipation. Note also that the experimental pressure signal has been low-pass filtered at 30$kHz$, which prevents the assessment of the numerical prediction of the high-frequency background noise. However, the latter is higher in LES than in DES, which is in agreement with the visualisations. Regarding the recycling method, the distance between the re-injection and the extraction planes would correspond, assuming advection at $U_\infty$, to a frequency of the order of 12$kHz$, which does not show up on the spectra, either in LES or DES. This confirms that the recycling technique has been applied sufficiently upstream, so that the spurious correlation it introduces has enough room to decrease before it reaches the cylinder.

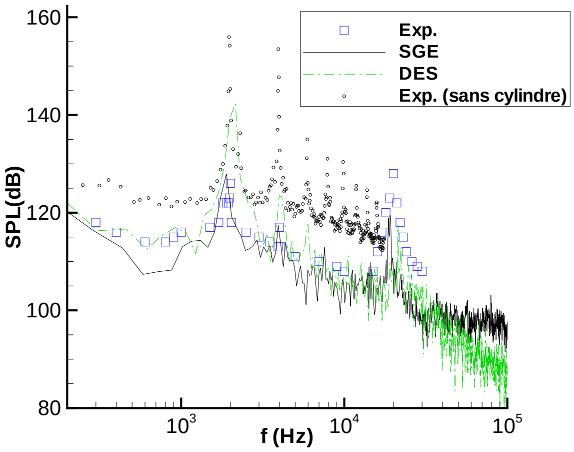

Figure 4: Pressure spectra at the rear wall of the cavity. Dark solid line: LES Pale solid line: DES. Small square symbols: baseline experiment (Forestier et al. 2003). Large square symbols: controlled configuration (Illy et al. 2004)

The effect of these upstream fluctuations is highly visible on the mean flow (Fig. 5): the recirculation length in LES is reminiscent of that of a freestream turbulent wake, whereas that in DES is about 3 times as large. It is well known that this recirculation length strongly depends on the turbulence level in the boundary layer of the cylinder, which determines the position of the separation points. As the Reynolds number, based on the cylinder diameter, is close to $4 \times 10^4$, the wake would be in the subcritical regime in free stream. However, the LES yields a drag coefficient of 0.48, rather reminiscent of the supercritical regime. We however cannot be conclusive regarding the accuracy of the treatment of the boundary layer of the cylinder, and can only notice the dramatic (and beneficial) effect of the injection of deterministic upstream fluctuations. The mean streamlines show a much less pronounced upward deviation of the meanflow in LES than in DES, with about the same additional thickening of the mixing layer due to the cylinder. This was not expected a priori, since the deviation and thickening of the mixing layer are considered as one of the possible explanations for the tone reduction caused by the cylinder (Ukeiley et al. 2002). Notice also that the baseline configuration (right plot of 5) exhibits a small recirculation bubble, analogous to that

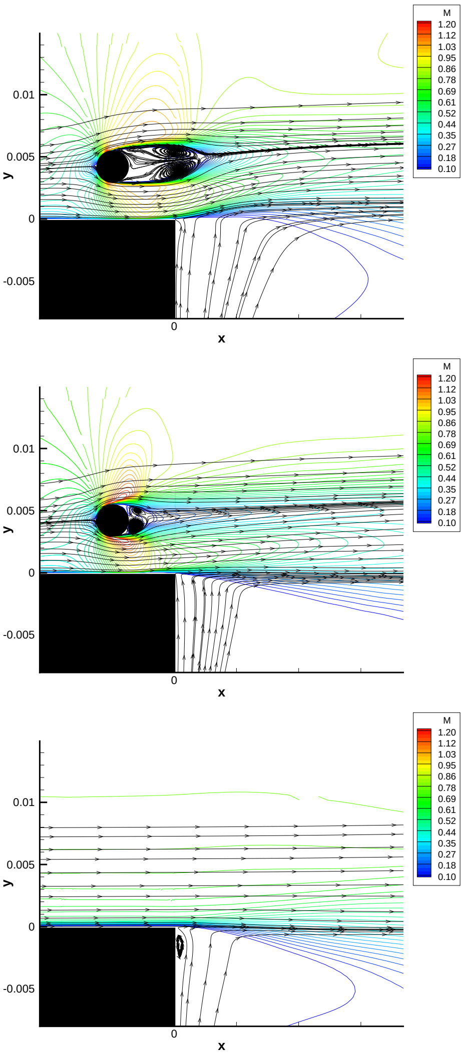

Figure 5: Mean streamlines iso-Mach number contours in the vicinity of the cylinder. From top to bottom: LES, DES, baseline.

observed at higher aspect ratio by (Larchevêque et al. 2004), who emphasized its possible importance in the feedback process. Although such a bubble is not visible in either the DES or the LES , the latter shows more attached mean streamlines around the upstream edge of the cavity, which is in favour of the argument in (Larchevêque et al. 2004).

The beneficial influence of the deterministic upstream perturbations is not outstandingly visible on the velocity statistics (Fig. 6). The mean velocity profiles are prescribed at $x = -50mm$ in both the DES and the LES. At $x = 0$ mm, above the fore edge of the cavity, that is, $5mm$ downstream of the cylinder's centerline, the turbulent kinetic energy and the Reynolds stress $u'v'$ (not shown here) in LES are correct, but the width of the wake is ever so slightly overestimated. The DES cannot build up the right turbulence level in such a short distance downstream of the cylinder. This was also the case in the DES of (Arunajatesan et al. 2002). Farther downstream ($x = 30$ and 40mm), the differences between DES and LES are less visible, but, with respect to the LDV measurements of (Illy et al. 2004), the LES tends to underestimate the wake's diffusion, whereas the DES overpredicts it.

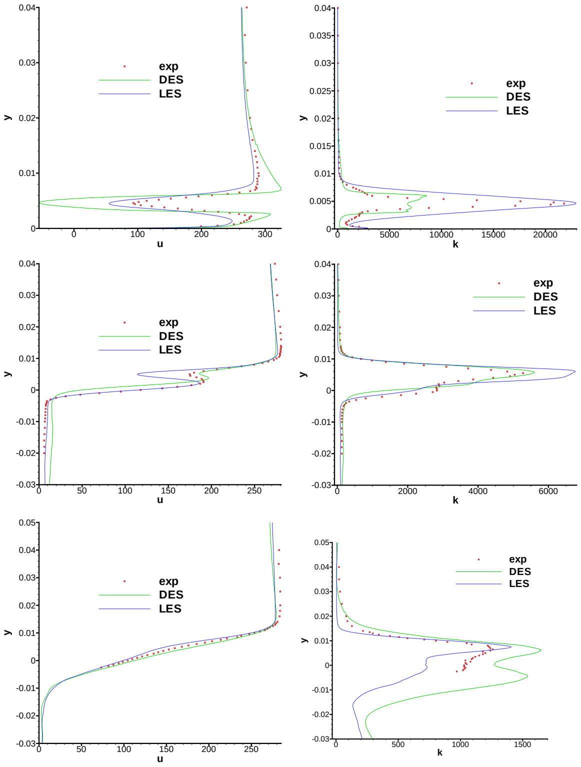

Figure 6: Profiles at at $x = 0$ mm, at $x = 10$ mm and at $x = 40$ mm (from top to bottom). Left row: mean velocity. Right row: resolved turbulent kinetic energy

The presence of locally supersonic regions, too mild to educe experimentally, was suspected in (Illy 2005) and (Illy et al. 2004). This is confirmed, not only by the mean Mach lines shown above, but also by instantaneous snapshots and movies, as in Fig. 7. This shows, in addition to Mach contours that indicate local Mach numbers beyond 1.8, and a positive Q surface, a Schlieren-type representation of density gradient conditioned by a high value of the dilatation, in order to educe the shocklets.

The upstream part of the supersonic region is found to be relatively stable, whereas its downstream part, in which the flow decelerates causing the shocklets, oscillates at the wake's shedding frequency. There is also visual evidence of merging between the Kelvin-Helmholtz-type vortices shed dowstream of the fore cavity edge and the lower row of von Kármán-type vortices shed behind the cylinder. This interaction takes place either immediately around $x = 0$, as in the bottom row of Fig. 7, or farther downstream during the other alternance of the wake shedding sequence, in which case the two vortical systems can clearly be distinguished before they merge.

One of the conjectures about the tone reduction is that the cylinder's wake reduces the 'breathing' of the cavity, namely, the variations of mass flow rate through its grazing plane, which is difficult to measure experimentally. This is shown here in Fig 8 from LES, in $(x, t)$ evolution after spanwise averaging (top row) and in time evolution only, after streamwise averaging (bottom row), over three periods of the fundamental Rossiter mode. In the baseline configuration, one can see about 10 in-out alternances per period near the fore edge, reduced to about 3 in the downstream quarter of the cavity, in a consistent fashion with the phase-averaged visualizations of (Larchevêque et al. 2003), in which the classical 'escaped, cut or trapped' sequence was educed with outstanding agreement between numerical results and PIV

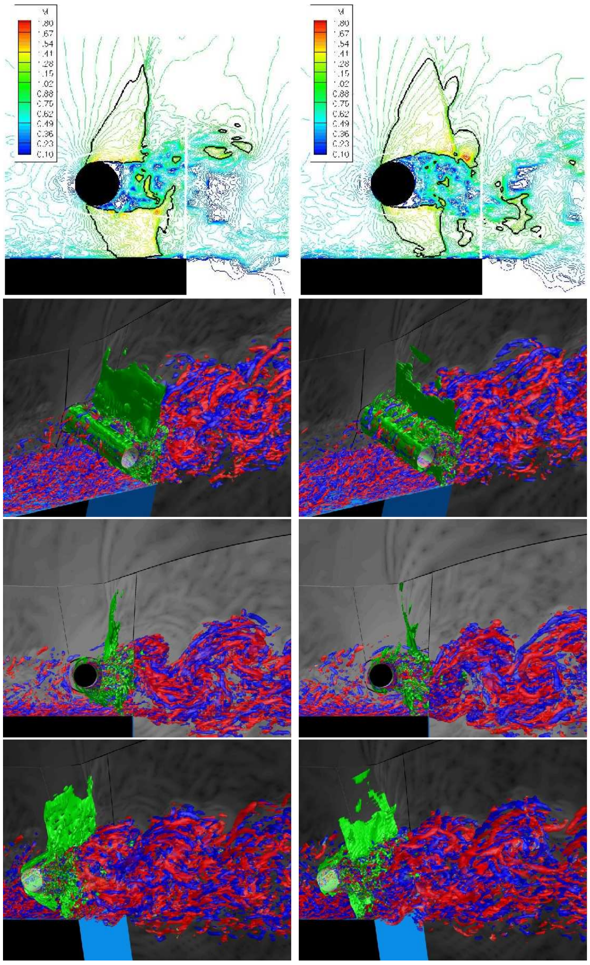

Figure 7: Iso Mach contours (left, with $M = 1$ contour emphasized) and isosurfaces of $Q = 2\ (U_\infty/d)^2$ coloured by the streamwise vorticity (blue/red), and of $|\partial_x \rho||\mathrm{div}\underline{u}| = 1.3\ d^2/(\rho_\infty U_\infty$ (green), at two instants of the cycle (left and right rows, resp.), in LES .

measurements. With the cylinder, the breathing amplitude is reduced by a factor of about 6, with more high frequencies and more alternances in the near fore edge region, close to the cylinder.

Kinetic energy and pressure spectra have been recorded along 5 constant $y$ mesh lines, for 50 periods of the fundamental Rossiter mode. Its frequency corresponds to $\log(2000)Hz$= 3.3 in Fig. 9, whereas that of the cylinder's wake is $\log(20000)Hz$= 4.3. The spectra at $y = 6mm$, not shown here, are very similar to those at $y = 3mm$ (recall that both $y$'s are symmetric *w.r.t.* the cylinder's centerline), which might indicate that the near wake itself responds to the Rossiter modes: indeed, the pressure spectra $y = 4mm$ show about $3dB$ less peak level at $\log f = 3.3$. In any case, above the grazing plane, the pressure peaks at $20kHz$ dominate those at $2kHz$, in contrast with those recorded inside the cavity (Fig. 9, right, and Fig. 4). At $y = 0$ and $y = -3mm$, we retrieve the node at $x = 0.5L$ of the first Rossiter mode observed in (Larchevêque et al. 2004) at higher aspect ratio. We also note 6 anti-nodes at $20kHz$ regularly spaced along $x$, which certainly correspond to a longitudinal acoustic mode of the cavity: indeed, considering a cavity with 5 walls yields, in the absence of a flow, $f_{n_x,n_y,n_z} = \frac{c}{2}\sqrt{\left(\frac{n_x}{L}\right)^2 + \left(\frac{n_z}{W}\right)^2 + \left(\frac{n_y+\frac{1}{2}}{D}\right)^2}$, hence, $n_x = \frac{2f_{n_x,0,0}L}{c} \sim 6$.

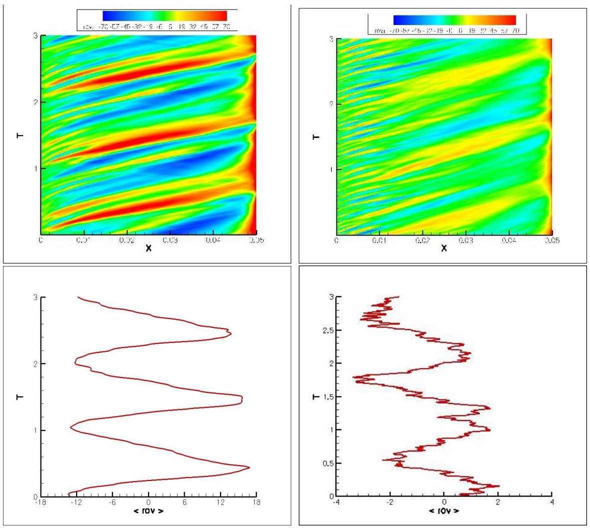

Figure 8: Evolution of the mass flow rate through the grazing plane: baseline configuration (left), LES with cylinder (right).

## CONCLUSION

Two hydrid RANS/LES calculations of the transonic flow over a cavity passively controlled by means of a spanwise rod are presented, and compared with the baseline configuration. The results are assessed with respect to the experimental measurements of Illy et al. (2004). With the cylinder dimensioned and position for maximal pressure tone reduction, a low $L/D$ aspect ratio is considered in order to minimize the complexity of the physics involved: in particular, the large-scale structure of the flow is quasi two dimensional, which makes it possible to use spanwise periodic boundary conditions. The simulations remain nonetheless quite computationally extensive ($\sim$ 2000 CPU hours per run), despite the adaptation of the numerics to the grid size variations required to capture both the incoming boundary layer and that which develops on the cylinder. In contrast with the baseline case, strong sensitivity of the nature of the upstream boundary layer fluctuations is found: indeed, in the absence of determininstic forcing, the wake of the cylinder is not turbulent enough to reduce the pressure tones to the experimental level, whereas an analogous simulation with deterministic fluctuations generated by recycling method is proved to be successful. The visualisations confirm that the impingement of Kelvin-Helmholtz-type vortices onto the aft edge of the cavity is indeed reduced, in agreement with Ukeiley et al. (2002). However, the two simulations do not show dramatic differences in the mean flow properties, and the mean upward deflection of the mean flow does not seem to be significant. Reduction of the amplitude of the mass flow rate 'breathing' through the grazing plane by a factor of 6 is observed *w.r.t.* the baseline case, together with the enrichment of the frequency content, due to additional small scales injected in the vicinity of the wake near the upstream edge of the cavity. This is in a sense consistent with the argument of Stanek et al. (2000), although analogous tone reduction

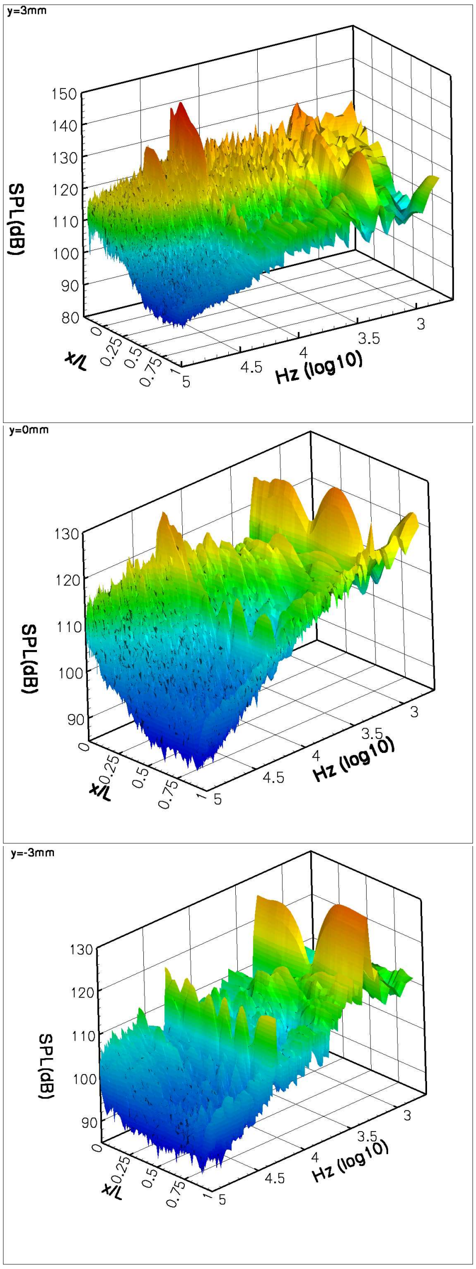

Figure 9: Streamwise evolution of the pressure spectra at $y = 3mm$, $y = 0mm$ and $y = -3mm$.

effects were observed by Illy (2005) at lower frequency ratio between the fundamental Rossiter mode and the wake shedding mode (here equal to 10). Finally, evidence of shocklets is provided, which was conjectured experimentally but difficult to measure.

## REFERENCES

Arunajatesan, S., Shipman, J. D., and Sinha, N., 2002, "Hybrid RANS-LES simulation of cavity flow fields with control". *AIAA Paper 2002-1130.*

Cattafesta, L. N., Williams, D. R., Rowley, C. W., and Alvi, F., 2003, "Review of active control of flow-induced cavity resonance". *AIAA Paper 2003-3567.*

Chatellier, L., Laumonier, J., and Gervais, Y., 2004, "Theoretical and experimental investigation of low mach number cavity flow". *Exp. Fluids*, 36:728–740.

Daude, F., Mary, I., and Comte, P., "Improvement of a Newton-based iteration strategy for the Large-Eddy Simulation of compressible flows". *submitted to J. Comp. Phys.*

Forestier, N., Jacquin, L., and Geffroy, P., 2003, "The mixing layer over a deep cavity at high-subsonic speed". *Journal of Fluid Mechanics*, 475:101–145.

Howe, M., 1997, "Edge, cavity and aperture tones at very low mach numbers". *J. Fluid Mech.*, 330:61–84.

Illy, H., 2005. *Contrôle de l'écoulement au-dessus d'une cavité en régime transsonique.* PhD thesis, École Centrale de Lyon, 2005.

Illy, H., Geffroy, P., and Jacquin, L., 2004, "Control of cavity flow by means of a spanwise cylinder". *21st ICTAM, Warsaw.*

Kravchenko, A. G., and Moin, P., 2000, "Numerical studies of flow over a circular cylinder at $Re_D = 3900$". *Physics of Fluids*, 12(2):403–417.

Larchevêque, L., 2003. *Simulation des Grandes Échelles de l'écoulement au-dessus d'une cavité.* PhD thesis, Université de Paris VI-Pierre et Marie Curie, 2003.

Larchevêque, L., Sagaut, P., Mary, I., Labbe, O., and Comte, P., 2003, "Large-eddy simulation of a compressible flow past a deep cavity". *Physics of Fluids*, 15(1):193–210.

Larchevêque, L., Sagaut, P., Lê, T.-H., and Comte, P., 2004, "Large-eddy simulation of a compressible flow in three-dimensional open cavity at high Reynolds number". *Journal of Fluid Mechanics*, 516:265–301.

Lenormand, E., Sagaut, P., Ta Phuoc, L., and Comte, P., 2000, "Subgrid-Scale Models for Large-Eddy Simulation of Compressible Wall Bounded Flows". *AIAA J.*, 38(8): 1340–1350.

Lund, T. S., Wu, X., and Squires, K. D., 1998, "Generation of Turbulent Inflow Data for Spatially-Developing Boundary Layer Simulations". *Journal of Computational Physics*, 140(2):233–258.

McGrath, S. F., and Shaw, L. L., 1996, "Active control of shallow cavity acoustic resonance". *AIAA Paper 96-1949.*

Powell, A., 1961, "On the edgetone". *J. Acoust. Soc. Am.*, 33:395–409.

Rockwell, D., and Naudascher, E., 1978, "Review: Self-sustained oscillations of flow past cavities". *ASME Journal of fluids engineering*, 100:152–165.

Rossiter, J. E., 1964, "Wind-tunnel experiments on the flow over rectangular cavities at subsonic and transonic speeds". *Aeronautical Research Council Reports and Memoranda*, 3438.

Rowley, C. W., and Williams, D. R., 2006, "Dynamics and control of high Reynolds-number flow over open cavities". *Ann. Rev. Fluid Mech.*, 38:251–276.

Stanek, M. J., Raman, G., Kibens, V., Ross, J. A., Odedra, J., and Peto, J. W., 2000, "Control of Cavity Resonance Through Very High Frequency Forcing". *AIAA Paper 2000-1905.*

Ukeiley, L. S., Ponton, M. K., Seiner, J. M., and Jansen, B., 2002, "Suppression of Pressure Loads in Cavity Flows". *AIAA Paper 2002-0661.*